



Holocene temperature fluctuations in the northern Tibetan Plateau

Cheng Zhao^{a,b,c,*}, Zhonghui Liu^a, Eelco J. Rohling^{b,d}, Zicheng Yu^c, Weiguo Liu^e, Yuxin He^a, Yan Zhao^f, Fahu Chen^f

^a Department of Earth Sciences, The University of Hong Kong, Hong Kong, China

^b School of Ocean and Earth Science, National Oceanography Centre, University of Southampton, Southampton SO14 3ZH, UK

^c Department of Earth and Environmental Sciences, Lehigh University, Bethlehem, PA 18015, USA

^d Research School of Earth Sciences, The Australian National University, Canberra ACT 0200, Australia

^e State Key Laboratory of Loess and Quaternary Geology, Institute of Earth Environment, Chinese Academy of Science, Xi'an 710075, China

^f MOE Key Laboratory of Western China's Environmental System, Research School of Arid Environment and Climate Change, Lanzhou University, Lanzhou 730000, China

ARTICLE INFO

Article history:

Received 23 November 2012

Available online 30 May 2013

Keywords:

Holocene

Climate variability

Arid Central Asia

Alkenones

ABSTRACT

Arid Central Asia (ACA) lies on a major climatic boundary between the mid-latitude westerlies and the north-western limit of the Asian summer monsoon, yet only a few high-quality reconstructions exist for its climate history. Here we calibrate a new organic geochemical proxy for lake temperature, and present a 45-yr-resolution temperature record from Hurleg Lake at the eastern margin of the ACA in the northern Tibetan Plateau. Combination with other proxy data from the same samples reveals a distinct warm–dry climate association throughout the record, which contrasts with the warm–wet association found in the Asian monsoon region. This indicates that the climatic boundary between the westerly and the monsoon regimes has remained roughly in the same place throughout the Holocene, at least near our study site. Six millennial-scale cold events are found within the past 9000 yr, which approximately coincide with previously documented events of northern high-latitude cooling and tropical drought. This suggests a connection between the North Atlantic and tropical monsoon climate systems, via the westerly circulation. Finally, we also observe an increase in regional climate variability after the mid-Holocene, which we relate to changes in vegetation (forest) cover in the monsoon region through a land-surface albedo feedback.

© 2013 University of Washington. Published by Elsevier Inc. All rights reserved.

Introduction

Climate in the Holocene, over the past 12,000 yr, has been characterized by gradual cooling in Northern Hemisphere high and mid-latitude areas and a drying trend in tropical/monsoon regions (Mayewski et al., 2004). This pattern is controlled by a gradual decrease in boreal insolation (Kutzbach and Street-Perrott, 1985; COHMAP Members, 1998). Superimposed on this long-term trend are several millennial-scale cooling events in high-latitude regions and/or drought or weak-monsoon events in tropical regions (O'Brien et al., 1995; deMenocal et al., 2000; Bond et al., 2001; Gupta et al., 2003; Mayewski et al., 2004; Wang et al., 2005). These millennial-scale events have been attributed to solar variability and/or internal ocean-atmosphere variations (Gupta et al., 2003; Mayewski et al., 2004; Wang et al., 2005).

Arid Central Asia (ACA) today falls under the influence of the mid-latitude westerlies. It marks the southern limit of a major source region of atmospheric dust, which affects the radiative forcing of climate on a global scale (e.g., Köhler et al., 2010; Roberts et al., 2011; Rohling et al., 2012). In a synthesis of eleven lake-sediment records

with relatively reliable chronologies and robust proxies, Chen et al. (2008) showed that Holocene climate in ACA experienced a gradual increase in humidity that was anti-phased with changes in the Asian monsoon region. However, other records for the late Pleistocene and Holocene indicate more complex and sometimes even opposite moisture changes within the ACA at various time scales (Lehmkuhl and Haselein, 2000; Yang et al., 2004; Yang and Scuderi, 2010; Yang et al., 2011). In the early Holocene, for instance, studies show that the climate around the boundary between the ACA and monsoon regions could be either dry (Mason et al., 2009) or wet (Yang et al., 2010) at different sites. In addition to the long-term trend, many lakes in the region have revealed major hydrological variations at millennial time-scales (Rhodes et al., 1996; Mischke et al., 2005; Mischke and Wünnemann, 2006).

Because of a dearth of paleoclimate records that give both temperature and moisture information from the same sites and same samples, understanding the nature of Holocene climate variability in the ACA is limited. Here we apply the new method for temperature reconstruction based on biomarker alkenone distributions in lakes to a sediment core from Hurleg Lake in the Qaidam Basin, northern Tibetan Plateau, to reconstruct a new quantitative temperature record for the ACA. Alkenones are produced by a limited number of haptophyte algae in the oceans and some lakes, and the ratio of different C₃₇-alkenone

* Corresponding author at: Department of Earth Sciences, The University of Hong Kong, Hong Kong, China.

E-mail address: C.Zhao@soton.ac.uk (C. Zhao).

compounds is very sensitive to temperature changes (Chu et al., 2005; Sun et al., 2007). A specific index, the alkenone unsaturation index or U^{K}_{37} (see below for details), is widely used for marine surface temperature reconstructions (e.g. Kim et al., 2004). However, recent culture experiments and studies of surface sediments from modern Chinese lakes have revealed that lakes also show a positive relationship between U^{K}_{37} values and surface water temperature, which in turn reflects air temperature (Chu et al., 2005; Sun et al., 2007; Chu et al., 2012). Here we present a statistical calibration with full propagation of uncertainties. We then develop a high-resolution (45 yr) quantitative temperature record for the last 9000 yr in Hurleg Lake (Fig. 1A). We combine this with information from other proxies (Zhao et al., 2010) to assess the long-term

orbital-scale trends, and millennial-scale climate variability around the Hurleg Lake region, and to test whether or not the monsoon influence expanded into the Qaidam Basin during the early-middle Holocene monsoon maximum.

Study site

Hurleg Lake and modern climate setting

The fresh-water lake, Hurleg Lake ($37^{\circ}17'N, 96^{\circ}54'E$; 2817 m above sea level [asl]) is located in the Qaidam Basin on the northern Tibetan Plateau (Fig. 1). The high surrounding mountains (~4000 m asl) are

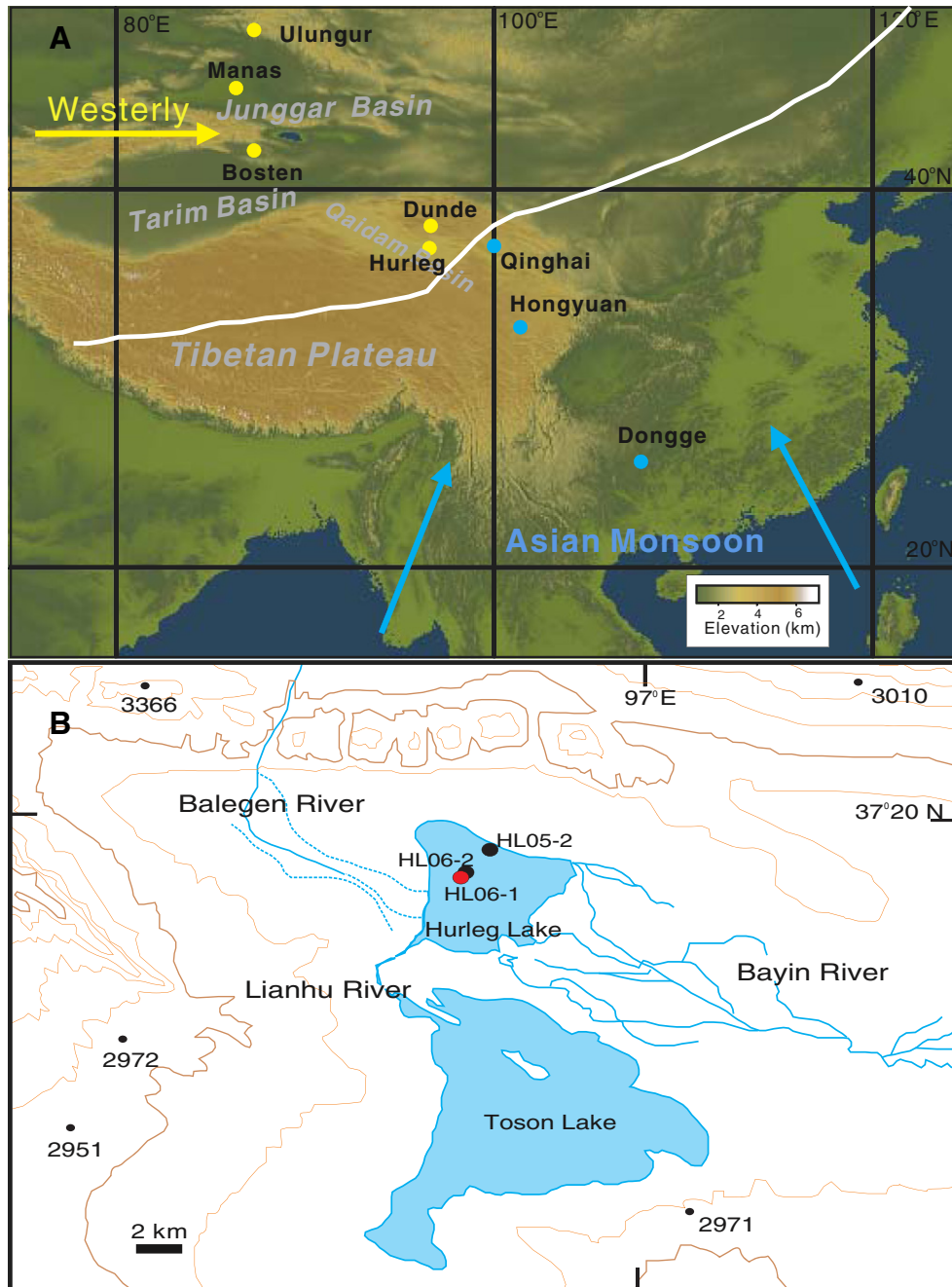


Figure 1. Location map. A. Hurleg Lake (yellow dot) is located in the northern Tibetan Plateau. Other sites mentioned include Lake Qinghai, Hongyuan Peat Bog, and Dongge Cave (blue dots) in the Asian monsoon region and Dundu Ice Cap, Bosten Lake, Manas Lake, Ulungur Lake (yellow dots) in westerly-dominated ACA. The bold white line approximately separates monsoon regions (blue) and ACA (yellow; after Chen et al., 2008). B. Topographic and hydrologic setting of Hurleg Lake. Red dot denotes the coring location for core HL06-1, and black dots indicate two other cores from the same lake (after Zhao et al., 2010).

influenced by the northern penetration of the Asian summer monsoon rainfall (Sheppard et al., 2004; Shao et al., 2005). The Qaidam Basin, however, currently lies just outside of the region of monsoonal rainfall (Tian et al., 2001, 2003) and is instead influenced by the mid-latitude westerlies (Fig. 1A; Chen et al., 2008).

Based on the instrumental data collected between 1956 and 2004 from Delingha station, the closest meteorological station about 30 km northeast of the lake, the mean annual air temperature (MAAT) is 3.7°C with a range from 1.6 to 5.2°C over the 48 year records. The seasonal mean air temperature varies from −9.7°C in winter (December, January, and February) to 15.6°C in summer (July, May, and August). The mean annual precipitation is ~160 mm with most falling in summer months. The mean annual potential evaporation is ~2000 mm (Yi et al., 1992). The vegetation is of a typical desert, dominated by Chenopodiaceae, *Artemisia*, *Ephedra* and *Nitraria* (Zhao et al., 2007). Based on multi-proxy evidence for the late Holocene, we have demonstrated that evaporation rather than inflow is the dominant cause of lake-level changes at Hurler Lake (Zhao et al., 2009, 2010).

Methods

Sample collection and lab analysis

Sediment cores HL06-1, HL05-2, and HL06-2 were obtained during field trips in summers of 2005 and 2006 (Fig. 1B). Both cores HL06-1 and HL06-2 were drilled in the lake center at about 7.6 m water depth (Fig. 1B) using a UWTEC corer. The 85-cm-long core HL06-2 was collected only 2 m away from core HL06-1 (Fig. 1B), as we noticed in the field that the core top of HL06-1 was lost. Based on our observations in the field, both cores (HL06-1 and HL06-2) show a clear lithological correspondence, and the top 27 cm was found to be missing from core HL06-1. The 688-cm-long core HL05-2 was collected at about 2.7 m water depth from a shallow part of the lake using a Livingstone–Wright piston corer (Fig. 1B). This study only focuses on core HL06-1. The 938-cm-long-core was subsampled at continuous 0.5–1 cm intervals. A total of 243 subsamples were analyzed for alkenones and alkanes following the standard procedure (Liu et al., 2011). Total lipids were obtained through extraction of freeze-dried sediments (about 2–6 g) with organic solvents, hydrolyzed to remove alkenoates that could interfere with the identification of alkenones, and then separated into three fractions with silica gel column chromatography. The alkenone and alkane fractions were analyzed by Gas Chromatography (Agilent 7890), using *n*-C₃₆ alkane as internal standard for quantification. The U^K₃₇ values were calculated using $U^{K}_{37} = C_{37:2} / (C_{37:2} + C_{37:3})$, where C_{37:2}, and C_{37:3} are the concentrations of di- and tri-unsaturated C₃₇ alkenones respectively. Analytical error is within 0.015 for U^K₃₇.

Dating and chronology

The chronology of core HL06-1 has been published previously (Zhao et al., 2010), based on seven AMS (accelerator mass spectrometry) ¹⁴C dates of aquatic plant leaves from *Ruppia* in core HL06-1, and four AMS ¹⁴C dates of the same material from parallel short core HL06-2 (Zhao et al., 2009, 2010). Based on the difference between paired ¹⁴C and ²¹⁰Pb dates at 12–13.5 cm from core HL06-2, all ¹⁴C dates were corrected by a constant 2758 ¹⁴C yr to account for the “old carbon” effect (Zhao et al., 2010). The corrected dates were calibrated using the Calib 5.0.1 program based on the IntCal04 calibration dataset (Zhao et al., 2010). Because the age model of Core HL05-2 was best approached by fitting a 3rd-order polynomial curve (Zhao et al., 2010), we here also apply 3rd-order polynomial curve for core HL06-1, using calibrated ages (Fig. 2). Two dating reversals and one date with a large deviation from the trend line were excluded from the age model. Uncertainties are presented by calculating two standard deviations for the scattering of individual dating points around the age model curve (Fig. 2A).

Although the required “old carbon” correction may in reality not be constant through time, it is currently difficult to assess this independently. However, the 2758 ¹⁴C-yr old-carbon correction we use here falls within the range of ¹⁴C reservoir ages (from a few hundred to 7000 ¹⁴C yr) for lakes across the Tibetan Plateau, according to a recent review (Hou et al., 2012). Still, when discussing millennial-scale climate variations, it is important to allow for a degree of (unknown) uncertainty in ages relative to dated events in other archives. We have aimed to minimize such impacts by: (1) always using the same material for dating (*Ruppia*); (2) comparing the inferred age model for HL06-1 with that of core HL05-2 from the shallower part of the lake to test reproducibility (Fig. 2); and (3) restricting the selection of samples for dating always to intervals with a narrow range of carbonate contents of about 30% to 40% to minimize changes in the relative admixture of old carbon.

U^K₃₇-temperature calibration and uncertainty estimation

Summer air temperature was calculated from the U^K₃₇ record based on a re-calibration ($U^{K}_{37} = 0.026T - 0.187$, $n = 38$, $R^2 = 0.40$) between U^K₃₇ data from modern sediments and summer air temperature at 38 Chinese lakes (Chu et al., 2005; Fig. 3). Uncertainties may exist in the U^K₃₇-temperature calibration from lakes in the natural environment, due to the potential influences of different producer species and lake chemistry (Chu et al., 2005; Toney et al., 2012). For this reason we validate the calibration using monospecific data from controlled culture experiments. In our re-calibration of the published data from Chu et al. (2005), uncertainties of both U^K₃₇ and temperature data are fully considered and propagated. All of the U^K₃₇ data for the calibration from 38 modern Chinese lakes have been considered with an analytical uncertainty of 0.006 (Chu et al., 2005). We consistently take the average of summer air temperature (June–July–August) over the same period between 1960 and 1993, and compute the standard deviation of summer air temperature over this 34-yr period as the uncertainty for temperature at each site. The calibration was determined by randomly perturbing all the data points in both the X (U^K₃₇) and Y (mean summer air temperature) directions 1000 times, according to normal distributions determined by the mean and error bars shown (Fig. 3). For each randomly perturbed realization, we performed a linear ordinary least-squares regression (using temperature as the independent variable). Next, we determined the median and the 2.5 and 97.5 percentiles of the complete set of 1000 regressions, to establish the calibration line and its 95% confidence limits.

We validate our U^K₃₇-temperature calibration for modern Chinese lakes with that from a culture experiment by Sun et al. (2007) and find that it reveals a virtually identical slope with the one from the culture experiment ($U^{K}_{37} = 0.026 * T - 0.261$, $n = 9$, $R^2 = 0.97$). That culture experiment concerned the haptophyte species *Chrysolita lamellosa*, collected from Lake Xiarinur, Inner Mongolia, China (Sun et al., 2007; Fig. 3). The alkenone producer in our study site Hurler Lake likely is the same (or closely related) species *C. lamellosa*, based on the following observations: (1) all our signals are C_{37:3} dominant rather than C_{37:4} dominant as found in some lakes from the USA that are produced by other species (Toney et al., 2012); (2) we did not detect any C_{38:3me} signals as shown in some USA lakes with different species (Toney et al., 2012); and (3) the waters of Lakes Hurler and Xiarinur are both dominated by anions of HCO₃⁻ and CO₃²⁻, rather than by sulfur, while the latter seems to specifically influence haptophyte species and alkenone production in lakes (Toney et al., 2012). Temperatures in the culture experiment refer to water temperature (Sun et al., 2007) rather than air temperature as in the modern-lake calibration (Chu et al., 2005), but previous studies indicate that lake surface temperature tends to be close to the ambient air temperature, especially for shallow lakes (Chu et al., 2005) like Hurler Lake. This would agree with our observation of an almost identical slope for both U^K₃₇-temperature calibrations from culture experiment and

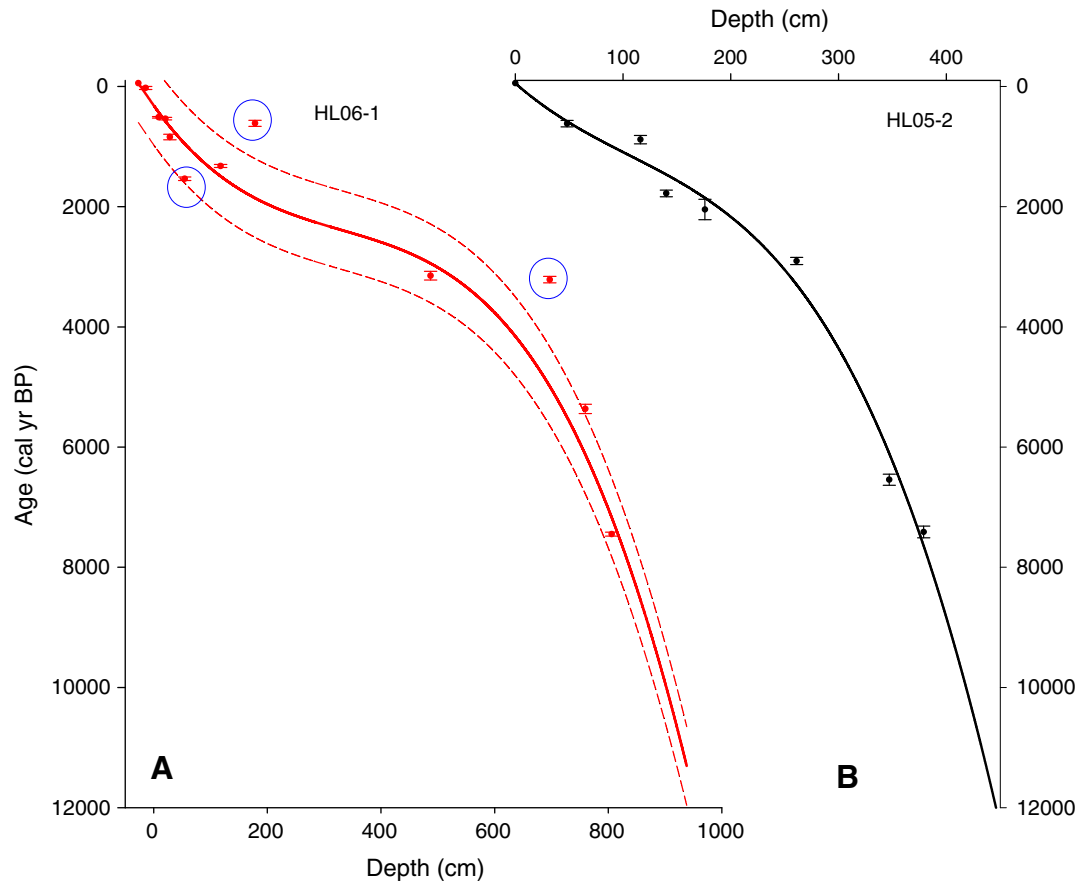


Figure 2. Chronology of sediment cores from Hurlig Lake. A. Age model for core HL06-1 based on a 3rd order-polynomial curve through corrected and calibrated AMS ^{14}C ages, four of which derive from the top parallel core HL06-2 (transferred to core HL06-1 on the basis of lithological correlation). Two dating reversals and one clear outlier were excluded from the model (blue circles). Red dashed lines represent 95% confidence limits. B. Age model of core HL05-2 from the shallow part of the lake, for comparison (Zhao et al., 2010).

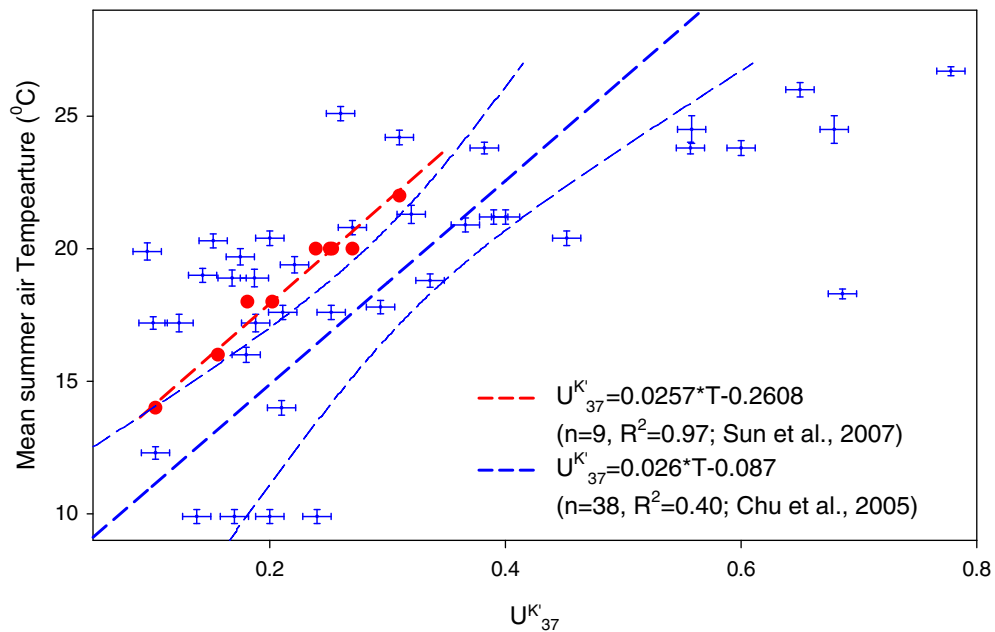


Figure 3. Calibration between U_{37}^K and summer air temperature with confidence limits. All data are from published studies as indicated in the figure. The blue data points represent the calibration from modern Chinese lakes (Chu et al., 2005). Each data point shows uncertainties (2-sigma error) in both directions. The bold blue dashed line is the regression line for all 38 data points. The thin blue dashed line indicates the 95% confidence level of the regression. The red dots show the calibration from culture experiments, with the red dashed line indicating the regression line (Sun et al., 2007).

modern Chinese lakes (Fig. 3). The only offset is in the intercept, suggesting that the equation of culture calibration would produce slightly higher temperatures than that of lake calibration. To highlight the changes in temperature through the Holocene and avoid any confusion about absolute temperatures due to different calibrations, we use only the calibration slope, to calculate summer air temperature variations relative to the calculated Holocene mean summer air temperatures from the entire record (ΔT). This ΔT will be independent and identical from both calibration equations (culture or lakes). Uncertainties of ΔT values are calculated from the uncertainties of lake calibration as shown in blue dashed lines in Fig. 3.

Results

Alkenone results for Hurlleg Lake sediments

The C_{37} -alkenone signals for the 243 samples analyzed from core HLO6-1 are divided into three categories (Fig. 4). Category 1 (138

samples) provides robust signals for temperature reconstruction (Fig. 4A). Category 2 (73 samples) contains C_{37} -alkenone concentrations that are too low to yield valid results (Fig. 4B). In the 32 samples of Category 3, we observe that the retention time of supposed compound $C_{37:3}$ signals consistently shifted behind that of the lab standard (Fig. 4C). GC-MS analyses confirm that Category-3 samples were contaminated by other organic compounds, which was also reported in Toney et al. (2012), and consequently they also fail to deliver robust results.

All Category-2 samples are from intervals before 9200 cal yr BP, around 4000 cal yr BP, 2900–2400 cal yr BP, and 1800–1200 cal yr BP (Fig. 5). These intervals generally have high long-chain (C_{27} – C_{33}) versus mid-chain (C_{21} – C_{25}) n -alkane ratios, extremely low alkenone concentrations of less than 10 ng/g, and low organic matter contents (Fig. 5). In addition, our previous work reveals low carbonate contents, high Ti counts, and low Ca/Ti ratios in these intervals (Fig. 6; Zhao et al., 2010). Category-3 samples are mainly from the intervals 4900–4300 cal yr BP, around 2000 cal yr BP, and 1100–600 cal yr BP (Fig. 5). These samples

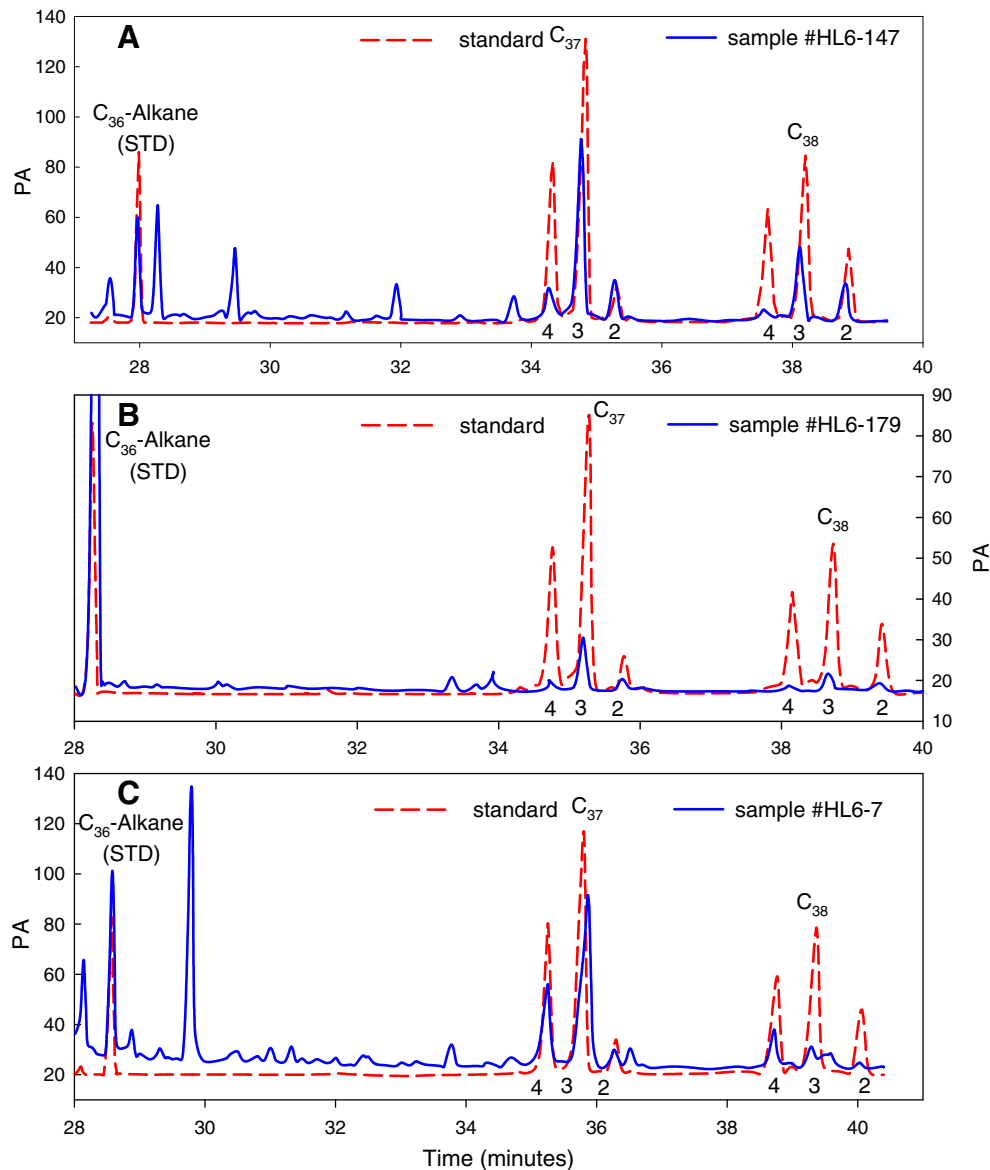


Figure 4. Alkenone signals from Hurlleg Lake. Blue curve: tested samples from Hurlleg Lake. Red dashed curve: alkenone standard in our laboratory. A. Robust signals (Category 1). B. Signals with very low C_{37} concentrations (Category 2), even though each sample has been concentrated 8 times. C. Compromised $C_{37:3}$ signals (Category 3). The $C_{37:3}$ -peak is delayed as compared to the laboratory standard, due to an unknown interfering compound, as has been confirmed by GC-MS analyses.

are generally associated with moderately low alkenone concentrations (10^1 – 10^3 ng/g), lower long-chain versus mid-chain *n*-alkane ratios, elevated organic matter and high carbonate contents, low Ti counts, and high Ca/Ti ratios (Figs. 5 and 6).

Relative to the 9300-yr mean value of 13.1°C based on modern Chinese lake calibration, or 16.1°C based on culture experiment calibration, our reconstruction for ACA reveals changes in summer air temperature (ΔT) between about -2.4 and 2.6°C over the past 9300 yr (Fig. 6A). Calibration uncertainties may range up to almost 2°C at 95% confidence level (Figs. 3, 6A), but the tight relationship seen in culture experiments (Fig. 3) suggests that the level of uncertainty inferred from our lake data calibration may be exaggerated. We distinguish six apparent millennial-scale cold events within the Holocene (Fig. 6A). A cold interval (ΔT at around -1 to -2°C), which commenced prior to 9000 cal yr BP, ended with a warming that culminated with ΔT at around $+2.6^\circ\text{C}$ between 8000 and 7000 cal yr BP. Values remained relatively high until about 6000 cal yr BP, followed by a sharp drop within a few centuries to cold conditions that culminated with ΔT at around -2.4°C by 5500 cal yr BP (Fig. 6A). After that, the record is more fragmented, but there are strong indications of sharp multi-centennial to millennial-scale fluctuations with ΔT between -1.6 and about $+2^\circ\text{C}$ (Fig. 6A).

Discussion

Multi-proxy evidence for Holocene moisture variations at Hurleg Lake

Long-chain *n*-alkanes are mainly produced by terrestrial plants, and mid-chain *n*-alkanes by aquatic plants (Meyers and Ishiwatari, 1993; Huang et al., 1999), so that Category-2 samples seem to be dominated by terrestrial plant material. This agrees with the low lacustrine productivity suggested by the low alkenone concentrations and organic matter contents. Based on our previously published data on modern lake sediment measurements and multiple down-core proxies, low carbonate concentrations, caused by enhanced dilution by silicate from the surrounding deserts during arid periods, suggest low lake levels (Zhao et al., 2010). Carbonate concentrations increase during times of high lake levels (Zhao et al., 2010), as supported by the Ti counts and Ca/Ti ratios from XRF data (Ca approximates the carbonate content, and Ti represents silicate abundance; Zhao et al., 2010). Taken together, it appears that Hurleg Lake experienced substantially lowered lake levels during the 'Category 2' intervals, due to relatively arid conditions. On the other hand, 'Category 3' intervals are similar to that for the modern freshwater condition, and suggest a relatively humid climate then (Fig. 5).

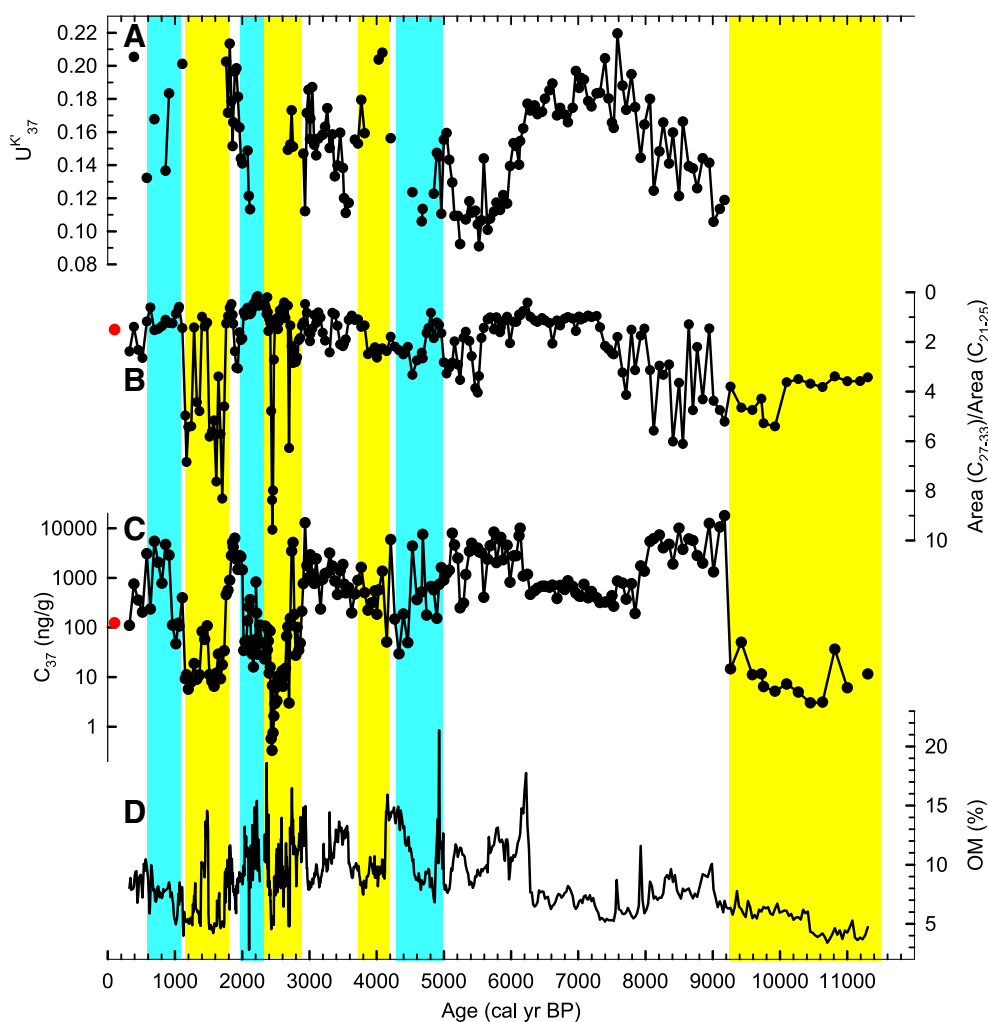


Figure 5. Multiple organic geochemistry-proxy records from Core HL06-1 at Hurleg Lake. A. U^K_{37} results. B. The ratios of Area (C_{27-33}) to Area (C_{21-25}), representing the relative abundance of terrestrial (long-chain) versus aquatic (mid-chain) alkanes (reversed scale). C. C_{37} -concentrations (in ng/g). In both B and C, filled red circles indicate results from a modern surface lake sediment sample. D. Organic matter (OM) percentage from loss-on-ignition analysis (Zhao et al., 2010). Yellow bands highlight extreme dry periods inferred from Category 2 samples, while blue bands highlight extreme wet periods inferred from Category 3 samples.

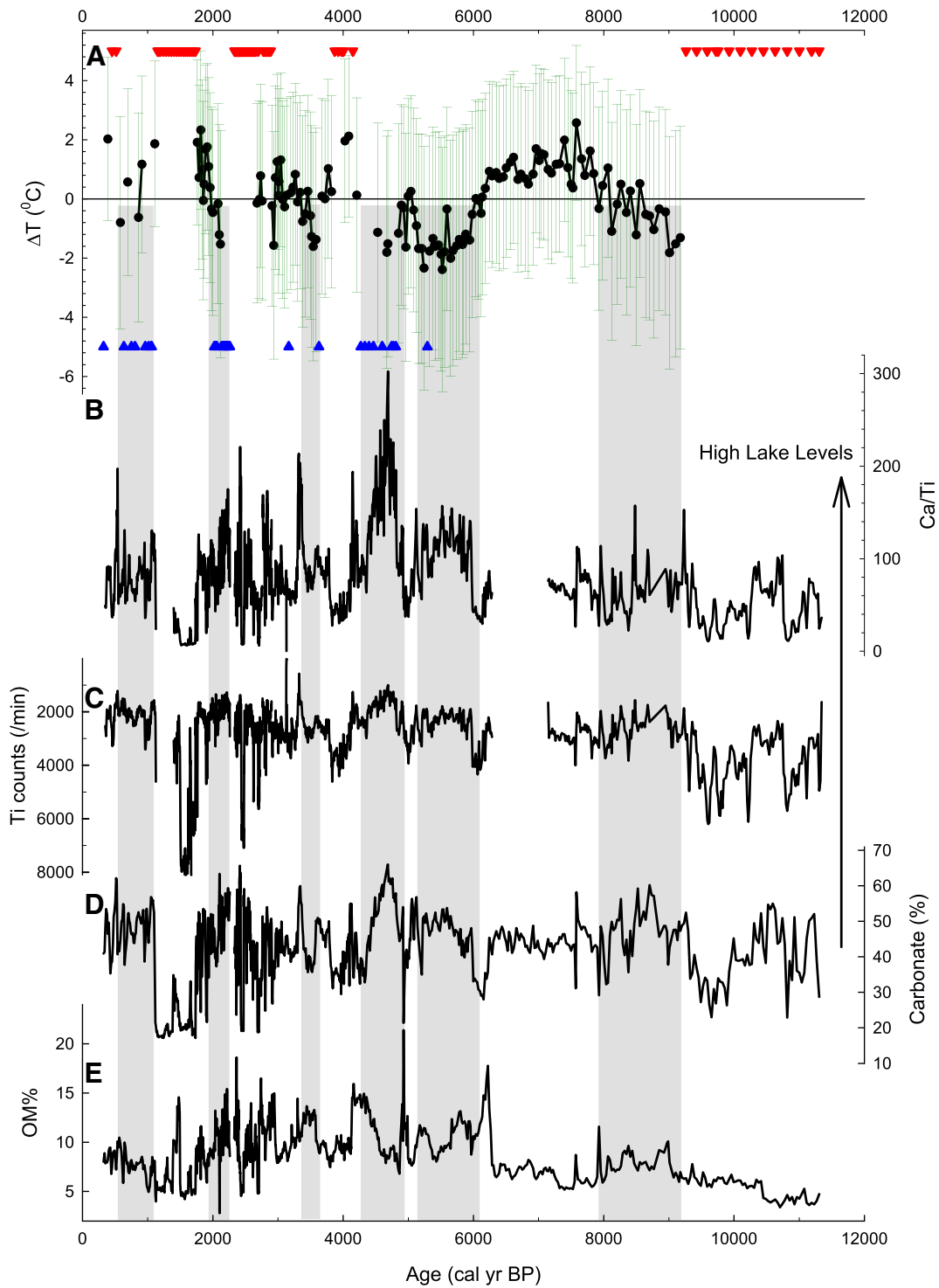


Figure 6. Holocene millennial-scale climate variability from core HL06-1 at Hurleg Lake. A. U^{K}_{37} -derived temperature record (ΔT) from Category-1 samples in Hurleg Lake with uncertainties (black dots and green error bars). The horizontal black line represents the mean over the past 9000 years. Red and blue triangles indicate the tentatively inferred temperature of Category-2 and -3 samples, respectively. B. Ca/Ti ratios from XRF analysis (Zhao et al., 2010). C. Ti counts from XRF analysis (Zhao et al., 2010). D. Carbonate content from loss-on-ignition analysis (Zhao et al., 2010). E. Organic matter content from loss-on-ignition analysis (Zhao et al., 2010). Gray shading represents six cold events based on our temperature reconstruction for Hurleg Lake.

Anti-phased millennial-scale moisture variations between ACA and monsoonal regions

Combined with other proxies (Fig. 6) from the same core samples (Zhao et al., 2010), our record suggests a warm-dry and cold-wet climate

associations in the Qaidam Basin. For instance, the relatively cold intervals at 9000–8000 cal yr BP and 6000–5100 cal yr BP coincided with high carbonate contents, high Ca/Ti ratios, and low Ti values (Fig. 6). Concomitant high organic-matter contents reflect elevated organic productivity during these colder intervals with high lake levels (Fig. 6E). Conversely, the

relatively warm interval at 8000–6000 cal yr BP is characterized by relatively low carbonate and low organic matter.

Based on the inferred warm–dry climate association in Category-1 samples, we infer that Category-2 samples with abundant indicators of aridity likely represent times of relatively warm conditions. Conversely, those from Category-3 samples with abundant indicators of enhanced humidity would represent relatively cool conditions. Possibly, intervals of Category-2 and -3 samples represent times of highly variable temperature and hydrological fluctuations that exceeded the recording capability of alkenone proxies (Liu et al., 2011). On this basis, we have tentatively added inferred ‘high’ and ‘low’ temperature indicators in Fig. 6A for Category-2 and -3 samples.

The ACA cold–wet climatic association on millennial timescales (Fig. 6) inferred from our Category-1 samples contrasts with the cold–dry association documented in nearby Lake Qinghai (Liu et al., 2006), which is affected by the monsoon climate (Fig. 1). Similar anti-phasing of hydrological changes between ACA and the monsoon regions has previously been suggested for the early Holocene (Chen et al., 2008; Mason et al., 2009) and for centennial-scale variations during the late Holocene (Yang et al., 2002; Zhao et al., 2009; Chen et al., 2010; Liu et al., 2010). This pattern has been attributed to a relationship between uplift of air in the monsoon areas and associated subsidence outside the monsoon region (Zhao et al., 2009), as supported

by simulations from numerical climate models (Sato and Kimura, 2005). Our data reveal that the warm–dry climatic association in the ACA, and hence the anti-phasing of moisture conditions between areas within and outside the current monsoon limit, have been persistent at millennial time scales throughout the past 9000 yr, at least near the study area. This implies that there have been no significant changes in the northward/westward penetration of the Asian monsoon through the course of the Holocene, at least near the northern Tibetan Plateau, which may provide a useful target for validating climate models.

Millennial-scale cold events and possible climate connection between North Atlantic and tropical Asian monsoon regions

The $\delta^{13}\text{C}$ time series of cellulose remains of sedges (*Cares mulieensis*) from the Hongyuan peat bog, eastern Tibetan Plateau, documents six weak monsoon events over the past 9000 yr (Fig. 7B; Hong et al., 2003). In southern China, similar weak monsoon events were documented in the $\delta^{18}\text{O}$ time series of a stalagmite from Dongge Cave (Fig. 7C; Wang et al., 2005). These weak monsoon events and associated aridity in the tropical Asian monsoon region have been previously related to the cold events in North Atlantic region (Hong et al., 2003; Wang et al., 2005). A synthesis of ~50 globally distributed paleoclimate records reveals six periods of rapid climate change during the past 9000 years, characterized by polar

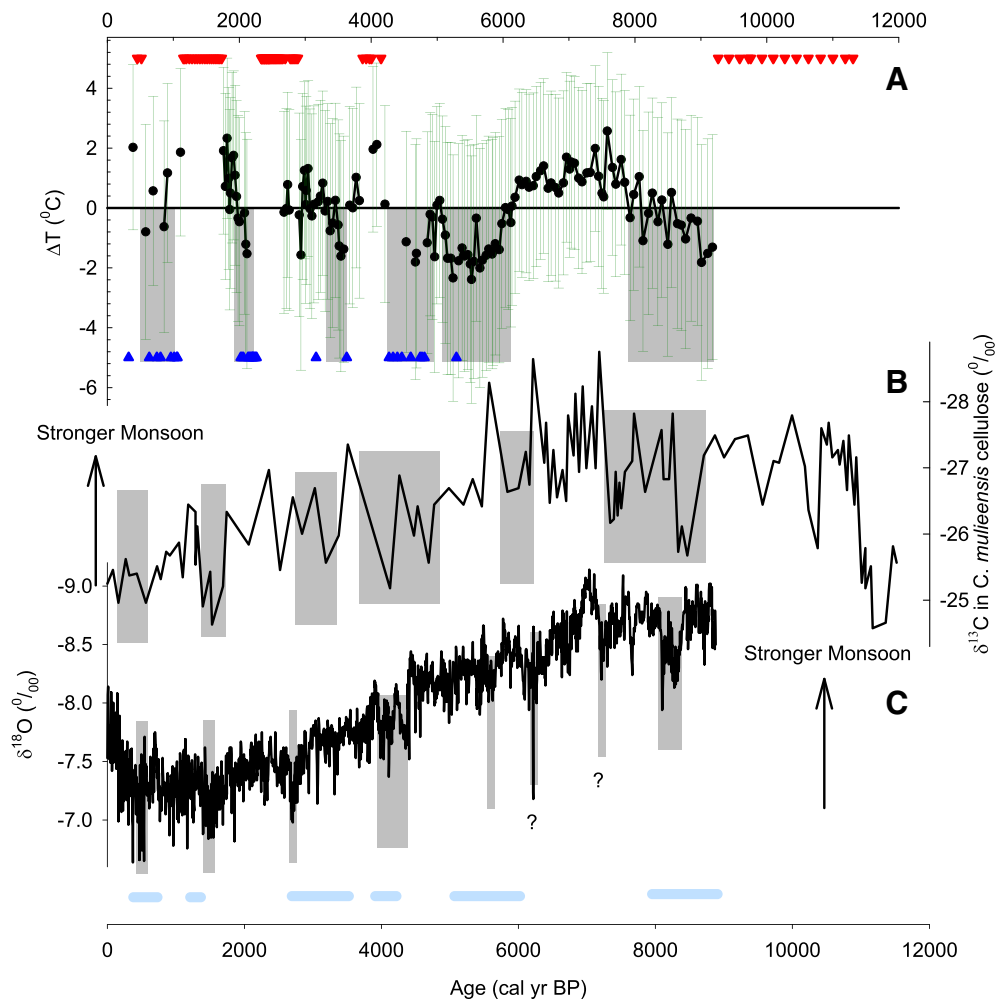


Figure 7. Correlation of millennial-scale climate variability. A. U^K_{37} -derived temperature record (ΔT) from Category-1 samples in Hurler Lake with uncertainties (black dots and green error bars). B. Carbon isotope record from Hongyuan peat bog as a proxy for Asian monsoon intensity (Hong et al., 2003). C. Oxygen isotope record from Dongge Cave as a proxy for Asian summer monsoon intensity (Wang et al., 2005). Gray bars indicate the cold intervals at Hurler Lake and the weak monsoon events as presented in each reference. The two with question marks (?) in C are only documented in the oxygen isotope record from Dongge Cave (Wang et al., 2005). Horizontal cyan bars at the bottom panel indicate six previously documented polar cooling and tropical drought events during the last 9000 years (Mayewski et al., 2004).

cooling and tropical aridity (blue lines in Fig. 7; Mayewski et al., 2004). In the 9000–5000 cal yr BP window, we have a coherent temperature proxy signal (Fig. 7A). Given the age uncertainties in our record (Fig. 2), we find millennial-scale cold events in Hurleg Lake that may correspond to the widespread polar cooling and tropical aridity intervals (Fig. 7) of Mayewski et al. (2004). After 5000 cal yr BP, the relationship is less clear, probably due to chronological uncertainties and fragmentation of our record due to an abundance of Category-2 and -3 samples (Fig. 7).

The Holocene weak monsoon and cold Atlantic events may reflect changes in either external forcing of solar output (Bond et al., 2001; Wang et al., 2005), or internal forcing of oceanic and atmospheric circulations (Gupta et al., 2003; Wang et al., 2005). If these events were initiated by solar forcing, then the millennial-scale cold events recorded in Hurleg Lake suggest that temperatures in the Asian continental interior were decreased during solar minima (Shindell et al., 2001), while the decreased thermal contrast between land and ocean may have reduced monsoon rainfall. If, in contrast, these events originated from the North Atlantic (Bianchi and McCave, 1999), then our data imply downwind propagation of the Atlantic cold events in the westerlies, along with decreased monsoon rainfall, as was also suggested in climate simulations by Feng and Hu (2008) and Sun et al. (2012).

Intensified millennial-scale climate variations in the ACA after the mid-Holocene

Our temperature record also suggests an increase in centennial- to millennial-scale variability after the mid-Holocene around 5000 cal yr BP (Fig. 8A). A similar increase in variability is seen in hydrological (Fig. 6) and biological (Fig. 5) proxies. The increased variability in many of these proxies could be caused by the increasing sedimentation rates from early to late Holocene, and we cannot fully exclude this possibility. However, the temperature record is derived by alkenone ratios between $C_{37:2}$ and $C_{37:3}$ rather than concentrations, and thus independent of the sampling resolution. In addition, the appearance of Category-2 and Category-3 alkenone signals after the mid-Holocene indicates an unprecedented variability of hydrological and ecological conditions in Hurleg Lake. Moreover, analysis of core HL05-2 from the same lake revealed increased variability in total pollen concentrations (Fig. 8b) as well as pollen percentages, including the terrestrial plants *Nitriaia*, Poaceae, *Artemisia*, Chenopodiaceae, and the aquatic algae *Pediastrum* (Zhao et al., 2007). Increased variability in the pollen data from Hurleg Lake reflects regional-scale climatic conditions in the Qaidam Basin (Zhao et al., 2007). At the Dundee ice cap (Fig. 1A),

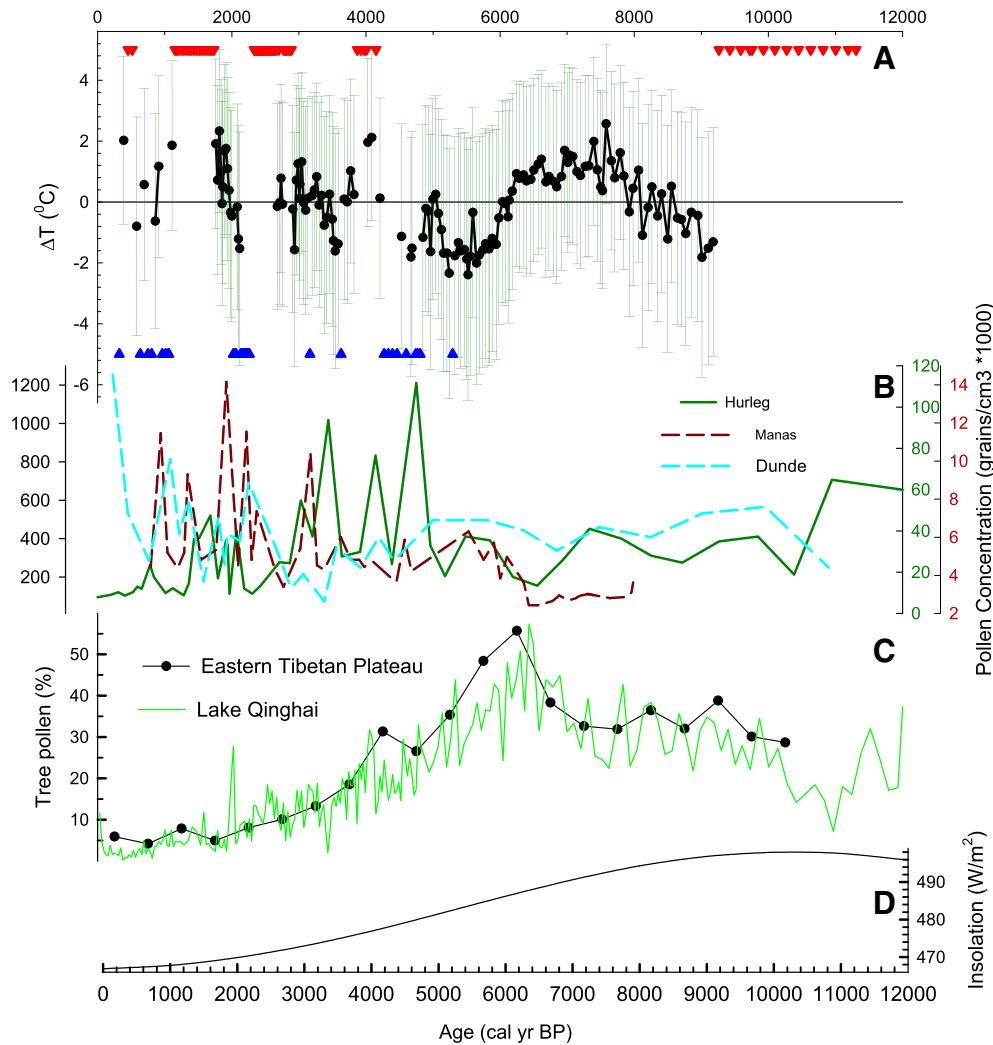


Figure 8. Shift in climate variability since the mid-Holocene. A. U^{K}_{37} -derived temperature record (ΔT) from Hurleg Lake. B. Pollen concentrations from Lake Manas (dashed brown curve; Rhodes et al., 1996), Dundee ice core (dashed cyan curve; Liu et al., 1998), and from core HL05-2 in shallow part of Hurleg Lake, which was published previously (dark green curve; Zhao et al., 2007; with updated chronology). C. Tree pollen percentages from Lake Qinghai (green curve; Shen et al., 2005) and synthesized tree pollen pattern (black line and dots) from the eastern Tibetan Plateau (Zhao et al., 2011). D. Summer insolation at 30°N (Laskar et al., 2004).

which is located in the ACA region but probably still influenced by monsoon precipitation (Davis et al., 2005) due to a much higher elevation, pollen concentrations also show an intensified variability during the mid- to late Holocene (Fig. 8B). This indicates more variable climate conditions in the surrounding areas (Liu et al., 1998) including the Qaidam Basin. Further to the northwest of Hurlig Lake, pollen data from Lake Manas (Fig. 1A) show similarly increased variability in pollen concentrations (Fig. 8B) during the mid-to late Holocene (Rhodes et al., 1996), indicating highly variable climate conditions in the Junggar Basin as well. In addition, the increased variability in total ostracode-shell concentrations (Jiang et al., 2008) from Ulungur Lake (Fig. 1A) and ostracode $\delta^{18}\text{O}$ values (Mischke and Wünnemann, 2006) from Bosten Lake (Fig. 1A) indicates higher variability in hydrological conditions at these lakes over the mid- to late Holocene. The increase in climate variability at the Qaidam Basin and other parts of the interior ACA after the mid-Holocene coincides with a major reduction of the hard-wood forest in the southern and eastern Tibetan Plateau from about 6000 to 4000 cal yr BP, as documented by pollen data (Fig. 8C) from Lake Qinghai (Shen et al., 2005) and other sites (Herzschuh et al., 2010; Zhao et al., 2011). This reduction likely relates to decreasing temperatures and rainfall in the monsoon region in response to the gradual decline in boreal summer insolation (Fig. 8D).

It has been suggested that the terrestrial biosphere has played a more prominent role in climate variability after the disappearance of large Northern Hemisphere ice sheets (Steig, 1999). Accordingly, we propose a potential link between the increased climate variability in our Hurlig Lake record and the climate/vegetation changes in nearby monsoon regions centered on 5000 cal yr BP. The insolation-related forest clearance and increase in barren lands would, through land-surface albedo feedbacks, have led to greater sensitivity to extremes at many sites within the ACA (Fig. 1).

Conclusions

We observe a generally opposite climatic association between arid Central Asia (warm and dry) and the Asian monsoon region (warm and wet) on millennial time scales. Based on its persistence throughout the Holocene, we infer that the northwestern limit of Asian summer monsoon penetration has not changed significantly throughout the Holocene, at least around our study site, despite the fact that the Asian monsoon was considerably intensified during the early Holocene and since then underwent a gradual reduction (An et al., 2000). Our quantitative temperature data reveal six millennial-scale cold events within the last 9000 yr in arid central Asia that may have correlated with previously documented cooling events in high to mid-latitude areas and weakened monsoons in tropical regions. This relationship is most evident in the uninterrupted portion of our record, between 9000 and 5000 cal yr BP, pointing at a possible connection between the North Atlantic and tropical monsoon system through the westerly circulation. Since the mid-Holocene, increased variability in key climate parameters and vegetation in the ACA suggests an intensified feedback relationship between vegetation, albedo, and climate due to the reduction of hardwood forest in the nearby monsoon region.

Acknowledgments

We thank J. Cao, A. Zhou, X. Liu and K. Zhang of Lanzhou University for field coring assistance; the Keck-CCAMS facility of University of California, Irvine for radiocarbon dating; the staff at LacCore (National Lacustrine Core Facility) of the University of Minnesota for initial core description and sub-sampling. The project was supported by the HK RGC (HKU 703809P) and HKU Stephen Hui Trust Fund (201103173003) to Z. Liu and Chinese NSF (NSFC #40528001) and US NSF (NSF EAR #0518774) to Z. Yu.

References

- An, Z., Porter, S.C., Kutzbach, J.E., Wang, X., Wang, S., Liu, X., Li, X., Zhou, W., 2000. Asynchronous Holocene optimum of the East Asian monsoon. *Quaternary Science Reviews* 19, 743–762.
- Bianchi, G.G., McCave, I.N., 1999. Holocene periodicity in North Atlantic climate and deep-ocean flow south of Iceland. *Nature* 397, 515–517.
- Bond, G., Kromer, B., Beer, J., Muscheler, R., Evans, M.N., Showers, W., Hoffmann, S., Lotti-Bond, R., Hajdas, I., Bonani, G., 2001. Persistent solar influence on North Atlantic climate during the Holocene. *Science* 294, 2130–2136.
- Chen, F., et al., 2008. Holocene moisture evolution in arid central Asia and its out-of-phase relationship with Asian monsoon history. *Quaternary Science Reviews* 27, 351–364.
- Chen, F., Chen, J., Holmes, J., Boomer, I., Austin, P., Gates, J.B., Wang, N., Brooks, S.J., Zhang, J., 2010. Moisture changes over the last millennium in arid Asia: a review, synthesis and comparison with monsoon region. *Quaternary Science Reviews* 29, 1055–1068.
- Chu, G., Sun, Q., Li, S., Zheng, M., Jia, X., Lu, C., Liu, J., Liu, T., 2005. Long-chain alkenone distributions and temperature dependence in lacustrine surface sediments from China. *Geochimica et Cosmochimica Acta* 69, 4985–5003.
- Chu, G., Sun, Q., Wang, X., Liu, M., Lin, Y., Xie, M., Shang, W., Liu, J., 2012. Seasonal temperature variability during the past 1600 years recorded in historical documents and varved lake sediment profiles from northeastern China. *The Holocene* 22, 785–792.
- COHMAP Members, 1998. Climate changes of the last 18,000 years: observations and model simulation. *Science* 241, 1043–1052.
- Davis, M.E., Thompson, L.G., Yao, T.D., Wang, N.L., 2005. Forcing of the Asian monsoon on the Tibetan Plateau: evidence from high-resolution ice core and tropical coral records. *Journal of Geophysical Research* 110, D04101. <http://dx.doi.org/10.1029/2004JD004933>.
- deMenocal, P., Ortiz, J., Guilderson, T., Sarnthein, M., 2000. Coherent high- and low-latitude climate variability during the Holocene warm period. *Science* 288, 2198–2202.
- Feng, S., Hu, Q., 2008. How the North Atlantic multidecadal oscillation may have influenced the Indian summer monsoon during the past two millennia. *Geophysical Research Letters* 35, L01707. <http://dx.doi.org/10.1029/2007GL032484>.
- Gupta, A.H., Anderson, D.M., Overpeck, J.T., 2003. Abrupt changes in the Asian southwest monsoon during the Holocene and their links to the North Atlantic Ocean. *Nature* 421, 354–357.
- Herzschuh, U., Birks, H.J.B., Liu, X., Kubatzki, C., Lohmann, G., 2010. Retracted: what caused the mid-Holocene forest decline on the eastern Tibet–Qinghai Plateau? *Global Ecology and Biogeography* 19, 278–286.
- Hong, Y.T., et al., 2003. Correlation between Indian Ocean Summer monsoon and North Atlantic climate during the Holocene. *Earth and Planetary Science Letters* 211, 371–380.
- Hou, J., D'Andrea, W.J., Liu, Z., 2012. The influence of ^{14}C reservoir age on interpretation of paleolimnological records from the Tibetan Plateau. *Quaternary Science Reviews* 48, 67–79.
- Huang, Y., Street-Perrott, F.A., Perrott, R.A., Metzger, P., Eglinton, G., 1999. Glacial-interglacial environmental changes inferred from molecular and compound-specific $\delta^{13}\text{C}$ analyses of sediments from Sacred Lake, Mt. Kenya. *Geochimica et Cosmochimica Acta* 63, 1383–1404.
- Jiang, Q., Shen, J., Liu, X., Zhang, E., 2008. Holocene climate reconstructions of Ulungur Lake (Xinjiang, China) inferred from ostracod species assemblages and stable isotopes. *Frontiers of Earth Science in China* 2, 31–40.
- Kim, J.H., Rimbu, N., Lorenz, S.J., Lohmann, G., Nam, S.O., Schouten, S., Ruhlmann, C., Schneider, R.R., 2004. North Pacific and North Atlantic sea-surface temperature variability during the Holocene. *Quaternary Science Reviews* 19, 171–187.
- Köhler, P., Bintanja, R., Fischer, H., Joos, F., Knutti, R., Lohmann, G., Masson-Delmotte, V., 2010. What caused Earth's temperature variations during the last 800,000 years? Data-based evidence on radiative forcing and constraints on climate sensitivity. *Quaternary Science Reviews* 29, 129–145.
- Kutzbach, J.E., Street-Perrott, F.A., 1985. Milankovitch forcing of fluctuations in the level of tropical lakes. *Nature* 317, 130–134.
- Laskar, J., Robutel, P., Joutel, F., Gastineau, M., Correia, A.C.M., Levrard, B., 2004. A long-term numerical solution for the insolation quantities of the Earth. *Astronomy and Astrophysics* 428, 261–285.
- Lehmkuhl, F., Haselein, F., 2000. Quaternary paleoenvironmental change on the Tibetan Plateau and adjacent areas (Western China and Western Mongolia). *Quaternary International* 65 (66), 121–145.
- Liu, K.B., Yao, Z., Thompson, L.G., 1998. A pollen record of Holocene climatic from the Dunde ice cap, Qinghai–Tibetan Plateau. *Geology* 26, 135–138.
- Liu, Z., Henderson, A.C.G., Huang, Y.S., 2006. Alkenone-based reconstruction of late-Holocene surface temperature and salinity changes in Lake Qinghai, China. *Geophysical Research Letters* 33, L09707. <http://dx.doi.org/10.1029/2006GL026151>.
- Liu, W., Liu, Z., An, Z., Wang, X., Chang, H., 2010. Wet climate during the 'Little Ice Age' in the arid Tarim Basin, northwestern China. *The Holocene* 21, 409–416.
- Liu, W., Liu, Z., Wang, H., He, Y., Wang, Z., Xu, L., 2011. Salinity control on long-chain alkenone distributions in lake surface waters and sediments of the northern Qinghai–Tibetan Plateau, China. *Geochimica et Cosmochimica Acta* 75, 1693–1703.
- Mason, J.A., Lu, H., Zhou, Y., Miao, X., Swinehart, J.B., Liu, Z., Goble, R.J., Yi, S., 2009. Dune mobility and aridity at the desert margin of northern China at a time of peak monsoon strength. *Geology* 37, 947–950.
- Mayewski, P.A., et al., 2004. Holocene climate variability. *Quaternary Research* 62, 243–255.
- Meyers, P.A., Ishiwatari, R., 1993. Lacustrine organic geochemistry – an overview of indicators of organic-matter sources and diagenesis in lake-sediments. *Organic Geochemistry* 20, 867–900.

- Mischke, S., Wünnemann, B., 2006. The Holocene salinity history of Bosten Lake (Xinjiang, China) inferred from ostracode species assemblages and shell chemistry: possible palaeoclimatic implications. *Quaternary International* 154–155, 100–112.
- Mischke, S., Demske, D., Wünnemann, B., Schudack, M.E., 2005. Groundwater discharge to a Gobi desert lake during Mid and Late Holocene dry periods. *Palaeogeography, Palaeoclimatology, Palaeoecology* 225, 157–172.
- O'Brien, S.R., Mayewski, P.A., Meeker, L.D., Meese, D.A., Twickler, M.S., Whitlow, S.I., 1995. Complexity of Holocene climate as reconstructed from a Greenland ice core. *Science* 270, 1962–1964.
- Rhodes, T.E., et al., 1996. A Late Pleistocene–Holocene lacustrine record from Lake Manas, Zunggar (northern Xinjiang, western China). *Palaeogeography, Palaeoclimatology, Palaeoecology* 120, 105–121.
- Roberts, A.P., Rohling, J.E., Grant, K.M., Larrasoana, J.C., Liu, Q., 2011. Atmospheric dust variability from Arabia and China over the last 500,000 years. *Quaternary Science Reviews* 30, 3537–3541.
- Rohling, E.J., Medina-Elizalde, M., Shepherd, J.G., 2012. Sea surface and high-latitude temperature sensitivity to radiative forcing of climate over several glacial cycles. *Journal of Climate* 25, 1635–1656.
- Sato, T., Kimura, F., 2005. Impact of diabatic heating over the Tibetan Plateau on subsidence over northeast Asian arid region. *Geophysical Research Letters* 32, L05809. <http://dx.doi.org/10.1029/2004gl022089>.
- Shao, X., Liang, E., Huang, L., Wang, L., 2005. A 1437-year precipitation history from Qilian Juniper in the Northeastern Qinghai–Tibetan Plateau. *PAGES News* 13, 14–15.
- Shen, J., Liu, X., Wang, S., Matsumoto, R., 2005. Palaeoclimatic changes in the Qinghai Lake area during the last 18,000 years. *Quaternary International* 136, 131–140.
- Sheppard, P.R., Tarasov, P.E., Graumlich, L.J., Heussner, K.U., Wagner, M., Österle, H., Thompson, L.G., 2004. Annual precipitation since 515 BC reconstructed from living and fossil juniper growth of northeastern Qinghai Province, China. *Climate Dynamics* 23, 869–881.
- Shindell, D.T., Schmidt, G.A., Mann, M.E., Rind, D., Waple, A., 2001. Solar forcing of regional climate change during the Maunder Minimum. *Science* 294, 2149–2152.
- Steig, E.J., 1999. Mid-Holocene climate change. *Science* 286, 1485–1486.
- Sun, Q., Chu, G., Liu, G., Li, S., Wang, X., 2007. Calibration of alkenone unsaturation index with growth temperature for a lacustrine species, *Chrysotila lamellosa* (Haptophyceae). *Organic Geochemistry* 38, 1226–1234.
- Sun, Y., Clemens, S.C., Morrill, C., Lin, X., Wang, X., An, Z., 2012. Influence of Atlantic meridional overturning circulation on the East Asian winter monsoon. *Nature Geoscience* 5, 46–49.
- Tian, L., Masson-Delmotte, V., Stievenard, M., Yao, T., Jouzel, J., 2001. Tibetan Plateau summer monsoon northward extent revealed by measurements of water stable isotopes. *Journal of Geophysical Research* 106, 28,018–28,088.
- Tian, L., Yao, T., Schuster, P.F., White, J.W.C., Ichiyangi, K., Pendall, E., Pu, J., Yu, W., 2003. Oxygen-18 concentrations in recent precipitation and ice cores on the Tibetan Plateau. *Journal of Geophysical Research* 108 (D9), 4293. <http://dx.doi.org/10.1029/2002JD002173>.
- Toney, J.L., Theroux, S., Andersen, R.A., Coleman, A., Amaral-Zettler, L., Huang, Y., 2012. Culturing of the first 37:4 predominant lacustrine haptophyte: geochemical, biochemical, and genetic implications. *Geochimica et Cosmochimica Acta* 78, 51–64.
- Wang, Y., Cheng, H., Edwards, R.L., He, Y., Kong, X., An, Z., Wu, J., Kelly, M.J., Dykoski, C.A., Li, X., 2005. The Holocene Asian monsoon: links to solar changes and North Atlantic climate. *Science* 308, 854–857.
- Yang, X., Scuderi, L., 2010. Hydrological and climatic changes in deserts of China since the Late Pleistocene. *Quaternary Research* 73, 1–9.
- Yang, X., Zhu, Z., Jaekel, D., Owen, L., Han, J., 2002. Late Quaternary palaeoenvironment change and landscape evolution along the Keriya River, Xinjiang, China: the relationship between high mountain glaciation and landscape evolution in foreland desert regions. *Quaternary International* 97 (98), 155–166.
- Yang, X., Rost, K.T., Lehmkuhl, F., Zhu, Z., Dodson, J., 2004. The evolution of dry lands in northern China and in the Republic of Mongolia since the last glacial maximum. *Quaternary International* 118–119, 69–85.
- Yang, X., Ma, N., Dong, J., Zhu, B., Xu, B., Ma, Z., Liu, J., 2010. Holocene hydrological and climatic changes in the Badain Jaran Desert, western China. *Quaternary Research* 73, 10–19.
- Yang, X., Scuderi, L., Paillou, P., Liu, Z., Li, H., Ren, X., 2011. Quaternary environmental changes in the drylands of China – a critical review. *Quaternary Science Reviews* 30, 3219–3233.
- Yi, X., Yang, D., Xu, W., 1992. China regional hydrogeology survey report-Toson Lake map (J-47-[25]) 1:200,000, Qaidam integrative geology survey, Golmud, Qinghai, China (in Chinese).
- Zhao, Y., Yu, Z., Chen, F., Ito, E., Zhao, C., 2007. Holocene vegetation and climate history at Hurlig Lake in the Qaidam Basin, northwest China. *Review of Palaeobotany and Palynology* 145, 275–288.
- Zhao, C., Yu, Z., Zhao, Y., Ito, E., 2009. Possible orographic and solar controls of Late Holocene centennial-scale moisture oscillations in the northeastern Tibetan Plateau. *Geophysical Research Letters* 36, L21705. <http://dx.doi.org/10.1029/2009GL040951>.
- Zhao, C., Yu, Z., Zhao, Y., Ito, E., Kodama, K.P., Chen, F., 2010. Holocene millennial-scale climate variations documented by multiple lake-level proxies in sediment cores from Hurlig Lake, Northwest China. *Journal of Paleolimnology* 44, 995–1008.
- Zhao, Y., Yu, Z., Zhao, W., 2011. Holocene vegetation and climate histories in the eastern Tibetan Plateau: controls by insolation-driven temperature or monsoon-derived precipitation changes? *Quaternary Science Reviews* 30, 1173–1184.